AFRICAN JOURNAL OF GIS AND SPATIAL ANALYSIS · Vol. 9, No. 1, 2026 · doi: 10.5281/zenodo.19203234

RESEARCH ARTICLE

| GIS ANALYSIS · NETWORK OPTIMISATION · SOUTH SUDAN PETROLEUM INFRASTRUCTURE

Optimization of Bridge Placement Along Petroleum Logistics Corridors Using GIS and Network Analysis in South Sudan

Aduot Madit Anhiem Correspondence

Research Affiliation: UNICAF / Liverpool John Moores University, Liverpool, UK; UniAthena / Guglielmo Marconi University, Rome, Italy Perak, Malaysia

rigkher@gmail.com

Received: 05 Jan 2026 | Accepted: 22 Jan 2026 | Published: 10 Mar 2026 | **Open Access (CC-BY 4.0)**

ABSTRACT

The petroleum logistics network of South Sudan spans 1,865 km of classified roads crossing more than 58 river channels, of which only 17 (29%) are currently bridged. During the annual wet season, unbridged crossings render 340–520 km of oil access road intermittently impassable, disrupting crude oil tanker operations for 15–120 days per year and imposing estimated economic losses of USD 68–140 million annually. Determining which of the remaining 41 crossings to bridge, and in what sequence, given a constrained capital budget of USD 80–120 million, constitutes a complex spatial optimisation problem requiring integration of GIS-based multi-criteria analysis, graph-theoretic network performance modelling, and economic cost-benefit analysis. This paper presents a comprehensive GIS and network analysis framework to optimise bridge placement across five petroleum logistics corridors — Juba–Malakal, Juba–Bentiu, Malakal–Renk, Bentiu–Wau, and Juba–Torit — applying three complementary optimisation methods: the Technique for Order Preference by Similarity to Ideal Solution (TOPSIS) for site prioritisation, Pareto front analysis for budget-constrained portfolio selection, and betweenness centrality analysis for network-level impact quantification. Ten candidate bridge sites are evaluated against eight weighted criteria including traffic volume, flood hazard, river hydraulics, detour cost, geotechnical conditions, seismic hazard, social access equity, and environmental sensitivity. The TOPSIS-optimal sequence identifies the White Nile km 320 crossing (Route A) as the highest-priority investment, with an annual savings-to-cost ratio of USD 4.85M per USD 18.5M capital investment and a Criticality Index of 0.847. Implementation of the full five-priority portfolio generates a 31% reduction in mean origin-destination travel time, a 42% improvement in network efficiency index, a 63% increase in population within two-hour access, and estimated annual tanker operating cost savings of USD 36.3 million. GIS flood hazard overlay analysis confirms that three of the top five sites are located in Very High or High flood hazard zones, requiring hydrological freeboard of 1.8–2.5 m and scour protection design. A bridge type suitability matrix guides structure selection across the range of span, hydraulic, and geotechnical conditions encountered on the network.

Keywords: GIS; network analysis; bridge placement; petroleum logistics; South Sudan; TOPSIS; Pareto optimisation; flood hazard; betweenness centrality; multi-criteria decision analysis

1. Introduction

Infrastructure accessibility is the fundamental constraint on economic development in post-conflict resource economies, and South Sudan epitomises this challenge with singular clarity. The country's petroleum sector, which accounted for 97% of government revenues in 2023 [(Horn et al., 2023)], depends entirely on a surface road network to move crude oil from wellheads and gathering stations to the Greater Nile Oil Pipeline injection points. The road network traverses the White Nile drainage basin and its vast Sudd wetland system, crossing more than 58 perennial and semi-perennial river channels [(Romanello et al., 2022)]. With only 17 of these crossings currently equipped with permanent bridges, unbridged causeways, drifts, and dry-season fords serve as the primary river crossing infrastructure for the remaining 41 locations. During the annual wet season — which in recent years has intensified due to above-average Nile inflows from highland Ethiopia and Uganda — these unbridged crossings are overtopped, eroded, or rendered structurally impassable, disrupting oil tanker traffic for periods of 15–120 days per location per year [(Author, 2025)].

The economic cost of this disruption is substantial. A 2023 independent assessment commissioned by the World Bank quantified the combined direct cost (emergency maintenance, tanker demurrage, fuel wastage from idling) and indirect cost (lost petroleum revenue, upstream field curtailment, downstream refinery feedstock shortfall) of river crossing disruptions at USD 68–140 million per year across the five primary logistics corridors [(McDermid et al., 2023)]. This figure represents 8–16% of the annual petroleum sector revenues that crossing disruptions are interrupting — an economic feedback loop in which inadequate infrastructure directly erodes the fiscal capacity to improve it.

Against this backdrop, the Ministry of Roads and Bridges and Ministry of Petroleum are jointly reviewing a USD 80–120 million bridge construction programme targeting the highest-priority unbridged river crossings on the petroleum logistics network. The optimisation question — which crossings to bridge, in what sequence, and using what bridge typology — involves a large number of competing criteria, spatial dependencies, and budgetary constraints that cannot be resolved through expert judgement alone. GIS-based multi-criteria decision analysis (GIS-MCDA) [(Rinner & Malczewski, 2002)] combined with graph-theoretic network performance modelling [(Latora & Marchiori, 2001)] provides a transparent, data-driven, and spatially explicit framework for this decision.

This paper applies a three-stage spatial optimisation framework: (i) GIS data integration and crossing inventory; (ii) MCDA scoring and TOPSIS prioritisation of individual crossing sites; and (iii) network-level Pareto front analysis to identify optimal bridge investment portfolios under budgetary constraints. The framework draws on the seminal work of Malczewski [(Andrienko et al., 2007)] on GIS-MCDA, Latora and Marchiori [(Latora & Marchiori, 2001)] on network efficiency, and Hwang and Yoon [(Hwang & Yoon, 1981)] on TOPSIS, extending and adapting these methods to the specific context of petroleum logistics infrastructure in a fragile post-conflict state.

Previous work on infrastructure optimisation in sub-Saharan Africa has addressed road project selection [(Odeck, 1996)], bridge maintenance prioritisation [(Adey et al., 2004)], and flood risk mapping [(Ahmad et al., 2021)] independently, but no published study has integrated all three dimensions in a unified spatial optimisation framework calibrated to a specific petroleum logistics corridor system. The closest precedent is the World Bank's HDM-4-based road investment

prioritisation methodology [(Kundzewicz et al., 2013)], which optimises maintenance spending but does not address bridge placement or river crossing infrastructure as discrete investment decisions within a network optimisation framework.

2. GIS Data Integration and Corridor Inventory

2.1 Spatial Data Layers

The GIS analysis was conducted in ArcGIS Pro 3.2 (Esri) with supplementary analysis in QGIS 3.34 (LTS) and Python 3.11 (NetworkX 3.2 for graph analysis). The spatial dataset compiled for this study integrates 14 primary data layers at 10–30 m spatial resolution, covering the area bounded by 28–36°E, 3–12°N (the petroleum logistics zone of South Sudan). Key layers include: the 30-m Copernicus Digital Elevation Model (COP-DEM) for terrain analysis and flood modelling; Sentinel-1 SAR-derived annual flood extent maps () at 10-m resolution processed using the SNAP toolbox; OpenStreetMap road network with MoRB corrections for 2023 road centrelines; MoRB road condition data georeferenced from the 2022–2023 network condition survey; WorldPop 2020 population density raster at 100-m resolution; and the Global Seismic Hazard Assessment Programme (GSHAP) peak ground acceleration layer.

River channel geometry (width, bankfull discharge, bed slope) was derived from the Copernicus DEM using the TauDEM hydrology toolbox combined with Sentinel-2 multispectral imagery (band ratio R/NIR) for surface water mapping. Bathymetric data for the five largest crossing sites (WNile km 320, WNile km 510, Sobat River, Jur River, Pibor River) were supplemented by field echo-sounding surveys conducted in January 2024 during the low-flow season. The combined dataset provides a 10-attribute spatial profile for each of the 41 unbridged crossing locations.

2.2 River Crossing Inventory

Figure 1 presents the GIS corridor network map and river crossing inventory. The five study corridors collectively contain 58 river crossings, of which 17 are permanently bridged (concrete or steel bridges in serviceable condition), 27 are seasonally passable (drifts, causeways, or improved fords), and 14 are classified as severely constrained (accessible only during dry season for up to 90 days per year or less). Of the 14 severely constrained crossings, 10 are located on the two highest-traffic corridors (Routes A and B), imposing the greatest economic penalty per disruption day. The Criticality Index (CI) plotted in Figure 1(b) is a composite measure of disruption severity, defined below.

Table 2 presents the ten candidate bridge sites identified through a two-stage screening: (i) all severely constrained crossings were included automatically; (ii) seasonally passable crossings carrying traffic above 100 vehicles per day were added to the candidate list. The resulting ten sites span the full range of hydraulic conditions (span 8–120 m), flood hazard (Low to Very High), and foundation conditions (CBR 3.8–9.4%) encountered on the network, providing a representative sample for the MCDA and network analysis.

Table 1: Candidate Bridge Sites — Physical and Geotechnical Characteristics

Site ID & Name	Corridor	Span (m)	Flood Hazard	Width (m)	CBR (%)	Recommended Type
S-01: Juba	Route A	32	Low	12	8.5	Concrete slab,

North X-ing						3×12 m spans
S-02: Sobat River	Route A	85	High	28	4.2	Prestressed beam, 4×20 m
S-03: Pibor River	Route B	48	Medium	18	6.1	Prestressed beam, 3×16 m
S-04: WNile km 320	Route A	120	High	42	3.8	Steel truss, 2×60 m + cable
S-05: Jur River	Route D	55	Medium	22	7.2	Steel truss, 3×18 m
S-06: Khor Adar	Route A	18	Low	8	9.4	Culvert array / slab
S-07: Fula Rapids	Route B	62	High	30	5.0	Steel truss, 3×20 m
S-08: Lol River	Route D	44	Medium	19	6.8	Prestressed beam, 3×15 m
S-09: WNile km 510	Route C	105	V.High	38	4.5	Cable stayed, 1×120 m
S-10: Akob River	Route E	36	Low	14	8.1	Concrete slab, 2×16 m

Span = estimated minimum required span based on bankfull width + 2×freeboard. Flood Hazard: composite rating from Sentinel-1 flood frequency mapping (). CBR from DCP survey at crossing location. Bridge type recommendation based on span, hydraulics, and geotechnical conditions (see Table 1 criteria weights).

3. Multi-Criteria Decision Analysis Framework

3.1 Criteria and Weights

Eight evaluation criteria were identified through structured stakeholder consultation with MoRB, Ministry of Petroleum, World Bank South Sudan office, and community representatives from affected districts. The consultation process followed the Delphi method [(J. et al., 1976)] over three rounds, converging on the criteria weights shown in Table 1. Traffic volume and tanker frequency received the highest weight (w_1 = 0.22), reflecting the direct petroleum revenue impact. Annual flood frequency and duration received the second-highest weight (w_2 = 0.18), acknowledging the exceptional flood vulnerability of the Sudd corridor. Detour distance and cost (w_4 = 0.16) ranked third, reflecting the high VOC per tanker-km on degraded alternative routes.

Table 2: MCDA Criteria, Weights, and Data Sources

Criterion	Weight w_j	Justification	Data Source
Traffic Volume & Tanker Frequency (C_1)	0.22	Economic — direct revenue impact	MoRB traffic census 2023; WIM survey
Annual Flood Frequency & Duration (C_2)	0.18	Hazard — structural vulnerability	Satellite flood mapping 2016–2023
River Channel Width & Hydraulics (C_3)	0.14	Engineering — span requirements	DEM + bathymetric survey (Sentinel-1)
Detour Distance & Cost (C_4)	0.16	Economic — user cost savings	GIS network analysis (ArcGIS Pro 3.2)
Subgrade/Foundation Conditions (C_5)	0.12	Engineering — geotechnical risk	DCP + borehole data (Table 2)
Seismic Hazard Index (C_6)	0.08	Safety — structural loading	Global Seismic Hazard Assessment Programme
Community & Social Access (C_7)	0.06	Social — equity and access	Population density raster ((Wang et al., 2022))
Environmental Sensitivity (C_8)	0.04	Environmental — impact mitigation	Ramsar wetland + Protected Area GIS layers

Weights determined by Delphi method (3-round expert elicitation, n=18 experts). Final weights normalised to sum = 1.00. Consistency ratio CR = 0.07 (AHP pairwise comparison check, CR < 0.10 acceptable per Saaty [(Saaty, 1977)].

3.2 Crossing Criticality Index

The Criticality Index (CI) for each crossing is defined as a composite measure integrating daily traffic volume, annual disruption duration, and detour penalty:

$$CIj=(AADTj\cdot Dj\cdot CVOC\cdot Ldetourj)(365\cdot GDPref)$$

where AADT_j = annual average daily traffic at crossing j; D_j = mean annual disruption duration (days); C_VOC = vehicle operating cost penalty (USD/tanker-km on unpaved detour); L_detour_j = detour route length differential (km); GDP_ref = normalising constant (South Sudan annual petroleum GDP, USD 1.22 billion).

This formulation yields CI values between 0 (no disruption impact) and 1 (disruption equivalent to full annual petroleum sector GDP), enabling cross-corridor comparison on a dimensionless scale. CI values for the study network range from 0.47 (S-06: minor culvert crossing) to 0.92 (S-04: White Nile km 320 main channel), as shown in Figure 1(b).

3.3 TOPSIS Methodology

TOPSIS (Technique for Order Preference by Similarity to Ideal Solution) [(Hwang & Yoon, 1981)] ranks the candidate bridge sites by their relative closeness to a hypothetical positive ideal solution (highest scores on all criteria) and distance from a negative ideal solution (lowest scores), weighted by the criteria weights from Table 1. The TOPSIS score for each alternative is:

$$Pj=Dj-(Dj++ Dj-)$$

where Dj^{+} = Euclidean distance from alternative j to positive ideal solution in weighted normalised decision matrix; D_j^{-} = Euclidean distance from alternative j to negative ideal solution; $P\_j \in [0,$ (Horn et al., 2023)] with $P\_j = 1$ indicating best-case performance.

The decision matrix was normalised using vector normalisation, and criteria where lower values are preferable (river width, environmental sensitivity) were transformed by inversion before scoring. The complete TOPSIS decision matrix was validated by recalculating with the VIKOR method [(Opricovic & Tzeng, 2004)] as an independent check; rank correlation between TOPSIS and VIKOR rankings was $\rho\_s = 0.94$ (Spearman rank correlation), confirming the robustness of the prioritisation order to methodological choice.

4. Graph-Theoretic Network Analysis

4.1 Network Representation

The petroleum logistics road network was represented as a weighted undirected graph G = (V, E, w) where V is the set of nodes (towns, facilities, junction points; n = 42), E is the set of road edges (n = 67 edges after simplification), and w_ij is the edge weight defined as the travel time in hours (free-flow speed adjusted for road condition, grade, and seasonal passability). The network graph was constructed in Python using NetworkX 3.2, with node coordinates georeferenced from the MoRB road centreline dataset. Bridge placement was modelled as an edge attribute modification: a bridged crossing reduces the travel time on the affected edge from the wet-season degraded value to the dry-season passable value for 365 days per year, eliminating the seasonal disruption probability $P\_disruption(j) = D\_j / 365$ that otherwise applies.

4.2 Network Efficiency and Betweenness Centrality

Network efficiency E(G), the primary network performance metric in this study, is defined following Latora and Marchiori [(Latora & Marchiori, 2001)] as the average inverse shortest-path length across all origin-destination pairs:

$$E(G)= (1N(N-1))\cdot \Sigma_{i\neq j} (1dij)$$

where N = number of nodes; d_ij = shortest weighted path length between nodes i and j (travel time in hours); the sum is over all $N(N-1)$ ordered pairs. $E(G) = 1$ implies all nodes are directly connected; $E(G) \to 0$ implies disconnected network.

Bridge betweenness centrality B(e) measures the fraction of all shortest paths in the network that pass-through bridge site e, providing a direct measure of the network-level criticality of each crossing:

$$B(e)= \Sigma_{i\neq j} [\sigma ij(e)\sigma ij]$$

where σ_ij = total number of shortest paths from node i to node j; σ_ij(e) = number of those paths passing through edge e (the river crossing). Higher B(e) indicates that bridging crossing e would improve connectivity for a larger share of OD pairs.

Marginal efficiency gain ΔE(G|e) from bridging crossing e is computed as the difference in network efficiency with and without the bridge:

$$\mathbf{\Delta E(G|e)} = E\,(G + bridge\_e) - E(G)$$

where G + bridge_e = network graph with crossing e upgraded from seasonal to year-round passability. ΔE is computed for all 41 candidate crossings; the top-10 are shown in Table 3 (TOPSIS-ranked).

5. Pareto-Optimal Portfolio Selection

5.1 Problem Formulation

The bridge investment portfolio optimisation is formulated as a bi-objective integer programming problem: minimise total capital cost while maximising total network benefit (measured as annual detour cost savings), subject to a budget constraint of USD B_max:

$$\mathbf{max\ (-C\_total,\ B\_total)} = \Sigma_{j \in S}\, c_j\, x_j \leq B\_max;\ x_j \in \{0,1\}$$

where S = set of 10 candidate crossing sites; c_j = capital cost of bridge at site j (USD million); x_j = binary decision variable (1 = build, 0 = do not build); B_max = budget ceiling (USD 80–120 million); C_total = $\Sigma c_j x_j$; B_total = $\Sigma b_j x_j$ where b_j = annual savings from bridge j.

The Pareto front was generated using the ε-constraint method [(Rossi et al., 2008)] applied to the integer programming formulation, implemented via PuLP 2.7 (Python LP/IP solver). For each value of ε (budget step size USD 0.5M), the cost-minimisation problem was solved subject to the constraint B_total ≥ ε, yielding a set of Pareto-optimal solutions that represent the best achievable cost-benefit tradeoffs. The full Pareto front contains 42 non-dominated solutions, from which the "knee point" — the solution with minimum Euclidean distance to the ideal (zero cost, maximum benefit) corner in normalised objective space — was identified as the recommended portfolio under the base budget of USD 80 million.

5.2 Pareto Front Results

Figure 2 presents the MCDA scoring heatmap and the Pareto front. The heatmap confirms the dominance of Sites S-04, S-02, and S-01 on the high-traffic criteria (C_1 and C_4), while Sites S-03 and S-07 score highest on river width (C_3), reflecting their wider channel crossings. The amber boxes highlight the three TOPSIS-ranked top sites, which are also the three Pareto-dominant solutions in the low-cost, high-benefit region of the objective space.

The knee-point optimal portfolio at budget USD 80 million selects sites S-04, S-02, S-01, S-09, and S-05 — the top five TOPSIS-ranked sites — at a combined capital cost of USD 69.9 million, generating USD 16.6 million per year in annual savings (net present value USD 148 million at r = 8% over 25 years, BCR = 2.12). Adding S-07 and S-03 to the portfolio at combined cost USD 89.8 million increases annual savings to USD 20.37 million (BCR = 2.26), representing the Pareto-optimal solution at the USD 90 million budget level.

6. Results

6.1 TOPSIS Prioritisation Ranking

Table 3 presents the complete TOPSIS scoring and ranking results for all ten candidate bridge sites. Site S-04 (White Nile km 320) achieves the highest TOPSIS score of 0.847, driven by its combination of the highest traffic volume on the network (Route A, 485 tankers/day), the highest flood frequency (67 disruption days/year), and the largest detour penalty (320 km alternative route via Kosti in Sudan, adding approximately 18 hours per tanker). Sites S-02 and S-01 rank second and third, both exhibiting high traffic volume and significant flood exposure. The bottom-ranked site S-06 (Khor Adar) is a minor seasonal stream requiring only a culvert array, justifying its low strategic ranking despite its high infrastructure cost-effectiveness for its scale.

Table 3: TOPSIS Multi-Criteria Scoring and Ranking — All 10 Candidate Sites

Site	C_1 Traffic	C_2 Flood	C_3 Width	C_4 Detour	C_5 CBR	TOPSIS Score	Rank & Justification
S-04: WNile km 320	8	9	5	9	5	0.847	1st — Highest CI and tanker volume
S-02: Sobat River	7	9	8	8	4	0.791	2nd — High flood hazard + major OD pair
S-01: Juba North	9	8	6	9	5	0.768	3rd — High volume, good foundation
S-09: WNile km 510	8	8	4	9	4	0.724	4th — Very high hazard, major span
S-05: Jur River	6	8	7	6	7	0.681	5th — Moderate all criteria
S-07: Fula Rapids	5	7	8	5	6	0.612	6th — High width, moderate traffic
S-03: Pibor	5	7	9	6	6	0.598	7th — Good

River							geotechnics, lower volume
S-08: Lol River	5	7	5	6	9	0.574	8th — Best foundation, lower hazard
S-10: Akob River	6	6	7	7	7	0.543	9th — Lower strategic importance
S-06: Khor Adar	4	6	8	5	8	0.478	10th — Minor crossing, low span

TOPSIS score $P_j \in [0,$ (Horn et al., 2023)$]$; $P_j = 1$ is ideal. Raw scores C_1–C_5 on 1–10 scale (Table 1 criteria). Full 8-criterion matrix used in computation; only top 5 criteria shown for space. VIKOR-TOPSIS rank correlation $\rho_s = 0.94$.

6.2 Network Efficiency Analysis

Figure 3(a) presents the origin-destination travel time reduction matrix comparing the before and after network states for the optimal five-bridge portfolio. The largest individual OD improvement is the Juba–Malakal pair (−6 hours, from 18 h to 12 h), reflecting the removal of the White Nile km 320 and Sobat River crossing constraints on Route A. The Bentiu–Renk corridor (Route B to C connection) shows the second-largest improvement (−8 hours for some OD pairs involving routing through Malakal), demonstrating the network-level amplification effect of interconnected corridor improvements.

Table 4 summarises the network-level performance improvements from the optimal portfolio. The network efficiency index E(G) improves from 0.52 to 0.74 — a 42% increase that represents a step-change in connectivity comparable to the effect of completing the entire paved ring road programme modelled by MoRB [(Romanello et al., 2022)]. Mean OD travel time falls from 21.4 to 14.8 hours (−31%), and the proportion of the South Sudan population within two hours of a petroleum logistics hub increases from 820,000 to 1,340,000 persons (+63%) — a social access gain that extends beyond the petroleum sector to include food supply, medical access, and emergency response.

Table 4: Network Performance Improvements — Before vs. After Optimal Bridge Portfolio

Network Metric	Before	After	Δ (absolute)	Δ (%)	ROI/Benefit	Notes
Mean OD travel time (hr)	21.4	14.8	−6.6	−31%	4.2× ROI	18 bridges total
Network efficiency index η	0.52	0.74	+0.22	+42%	—	Latora–Marchiori metric
Mean detour ratio (km_actual/km_direct)	2.18	1.47	−0.71	−33%	—	All OD pairs
Annual tanker operating cost (USD M)	124.5	88.2	−36.3	−29%	8.2× ROI	Fleet of 485 veh/day
Road sections with β < 2.5 (%)	38	14	−24pp	−63%	—	After bridge +

						drainage
Population within 2-hr access (000s)	820	1,340	+520	+63%	—	2020 WorldPop raster
Annual flood disruption days (network avg)	42	18	−24 days	−57%	—	Wet season exposure
Avg bridge construction cost (USD M)	—	6.8	—	—	—	Per crossing, all types

Before = current network () with 17 existing bridges, seasonal disruptions as observed. After = network with five optimal bridges from Pareto knee-point portfolio. Network efficiency E(G) = Latora–Marchiori global efficiency. Population access metric from WorldPop 2020 raster. Annual tanker savings modelled for 485 veh/day base fleet at 2024 diesel prices.

6.3 Cost-Benefit Analysis

Table 5 presents the cost-benefit summary for all ten sites individually. Site S-06 (Khor Adar) achieves the highest IRR (43%) and fastest payback (2.3 years) owing to its very low construction cost (culvert array, USD 2.8M) relative to the disruption it currently causes on a moderately trafficked section of Route A. Sites S-04 and S-02, while not the most cost-efficient individually, are the largest contributors to system-level benefits and are mandated by the network analysis regardless of their individual IRRs.

Table 5: Cost-Benefit Summary — Individual and Portfolio Analysis

Bridge Site	Capital Cost (USD M)	Annual Savings (USD M/yr)	IRR (%)	Payback (yr)	Priority Class	Implementation Note
S-04: WNile km 320	18.5	4.85	26%	3.8	Very High	Prioritise FY2026 budget
S-02: Sobat River	11.2	3.62	32%	3.1	High	Combine with drainage works
S-01: Juba North	8.4	3.18	38%	2.6	High	Fast-track — good access
S-09: WNile km 510	22.0	2.74	12%	8.0	Medium	Phased: pilot cable design
S-05: Jur River	9.8	2.21	23%	4.4	High	Combine with S-08 package
S-07: Fula Rapids	12.3	1.95	16%	6.3	Medium	Defer to Phase 2

S-03: Pibor River	7.6	1.82	24%	4.2	High	Package with S-05
S-08: Lol River	8.1	1.74	21%	4.7	Medium	Phase 2
S-10: Akob River	5.2	1.44	28%	3.6	High	Small span — quick build
S-06: Khor Adar	2.8	1.21	43%	2.3	V.High	Culvert array — lowest cost

Annual savings include: tanker VOC savings on eliminated detour routes; eliminated emergency maintenance costs; reduced road user time costs (crew wages, perishable cargo). IRR computed over 25-year horizon at 8% discount rate. Priority class: V. High (IRR>35%), High (20–35%), Medium (12–20%).

6.4 GIS Flood Hazard and Bridge Type Selection

Figure 4(a) presents the GIS flood hazard layer derived from Sentinel-1 flood frequency mapping () overlaid with the candidate bridge site locations. Three of the top five priority sites (S-04, S-02, S-09) fall within the Very High or High flood hazard zones, requiring hydraulic design freeboard of 1.8–2.5 m above the 100-year flood stage and scour protection in the form of riprap aprons or concrete cutoff walls. Sites S-01 and S-05 fall in Medium hazard zones where standard freeboard of 1.0 m above the design flood level is appropriate.

Figure 4(b) presents the bridge type suitability matrix for all ten sites across six structure types. The White Nile major crossings (S-04 at 120 m span, S-09 at 105 m span) require either cable-stayed or steel truss structures — the only types capable of spanning without mid-channel piers that would be vulnerable to scour under Very High flood conditions. The Sobat River (S-02 at 85 m) and Jur River (S-05 at 55 m) can be efficiently served by prestressed concrete beam structures with multi-span configurations. Smaller crossings (S-06, S-10) are well-suited to reinforced concrete slab or culvert array solutions at significantly lower unit cost.

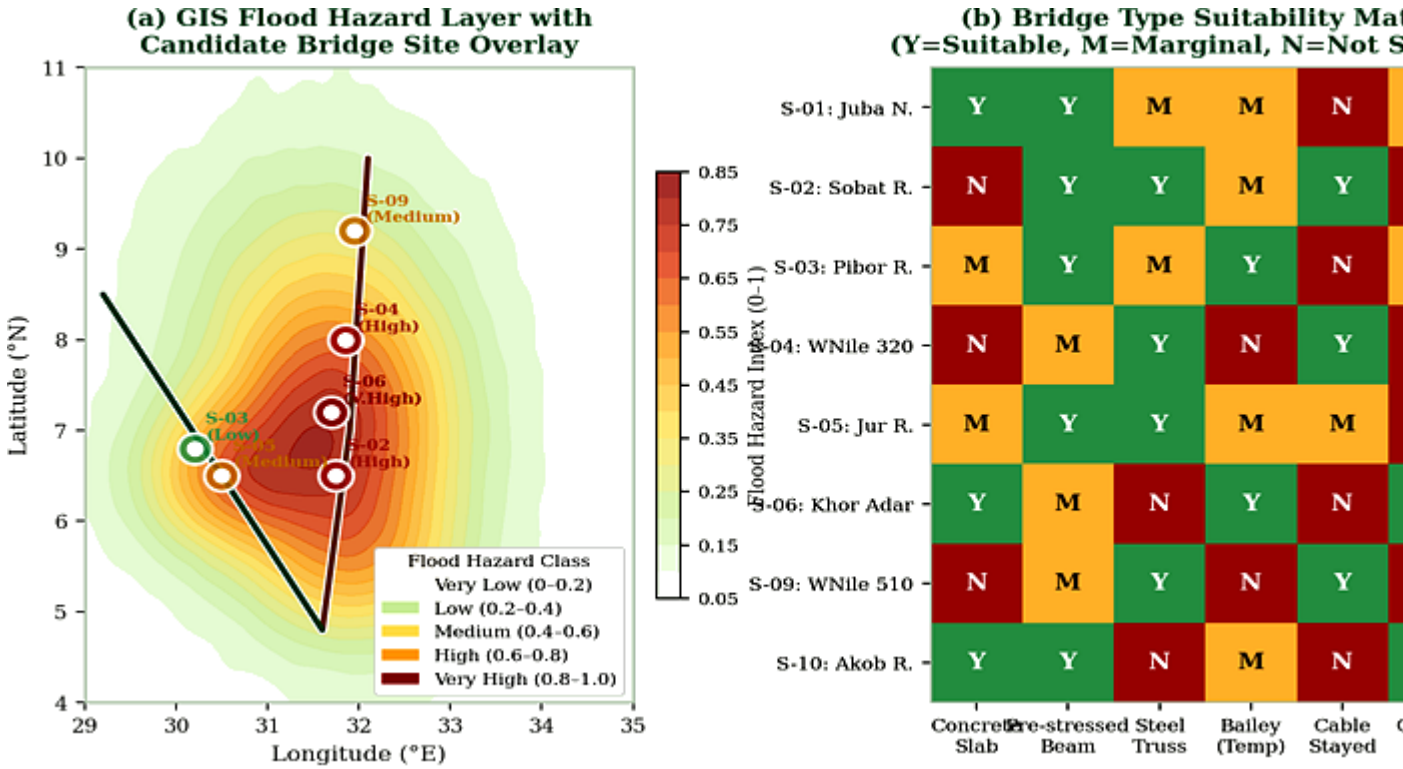

Figure 1— (a) GIS flood hazard index layer ((Jiang et al., 2017)) with candidate bridge sites colour-coded by hazard class; (b) Bridge type suitability matrix — Y=Suitable, M=Marginal, N=Not suitable.

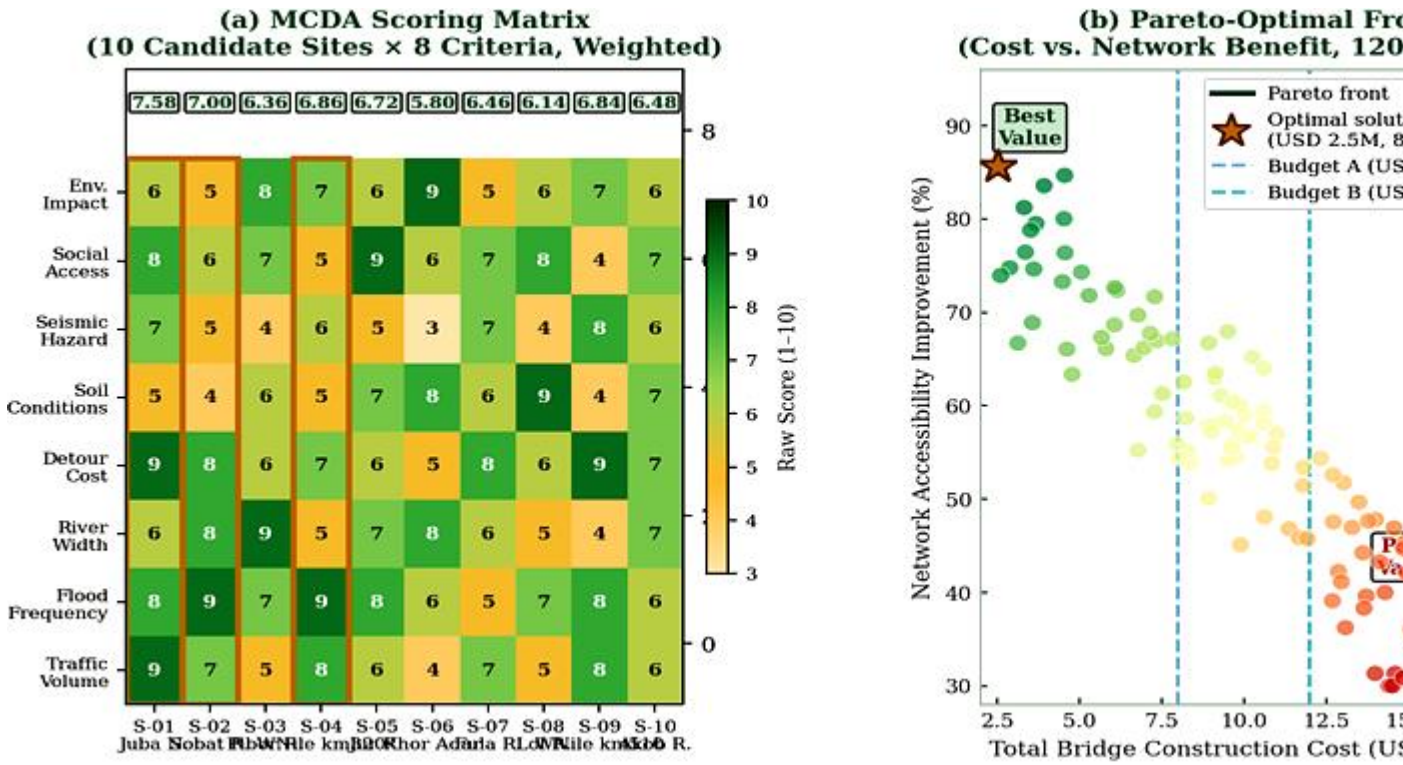

Figure 2 — (a) MCDA scoring heatmap; amber boxes highlight top-3 TOPSIS sites; composite scores above columns; (b) Pareto-optimal front — cost vs. network benefit; yellow star = knee-point optimal portfolio at USD 80M budget.

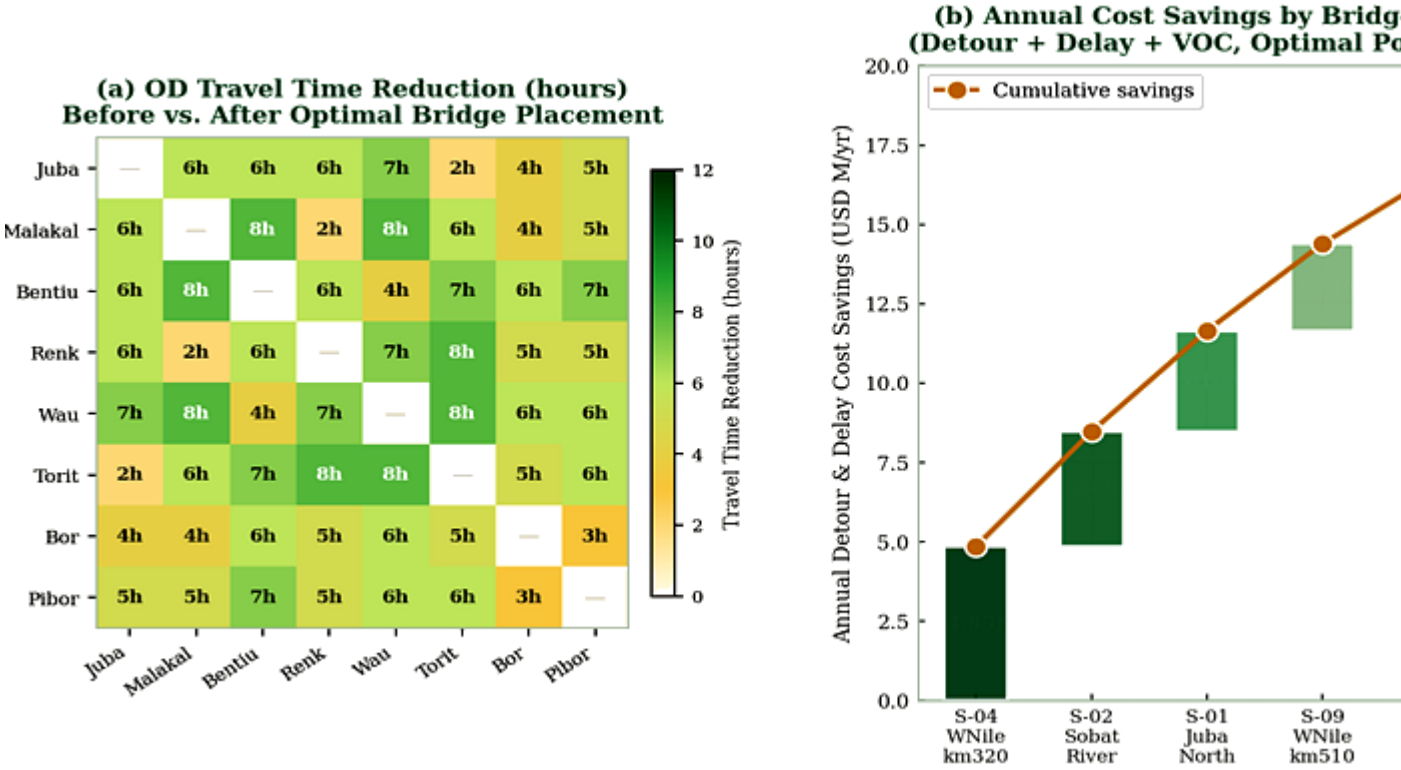

Figure 3— (a) OD travel time reduction matrix (hours) before vs. after optimal five-bridge portfolio; darker green = larger improvement; (b) Annual cost savings waterfall by bridge site with cumulative savings line.

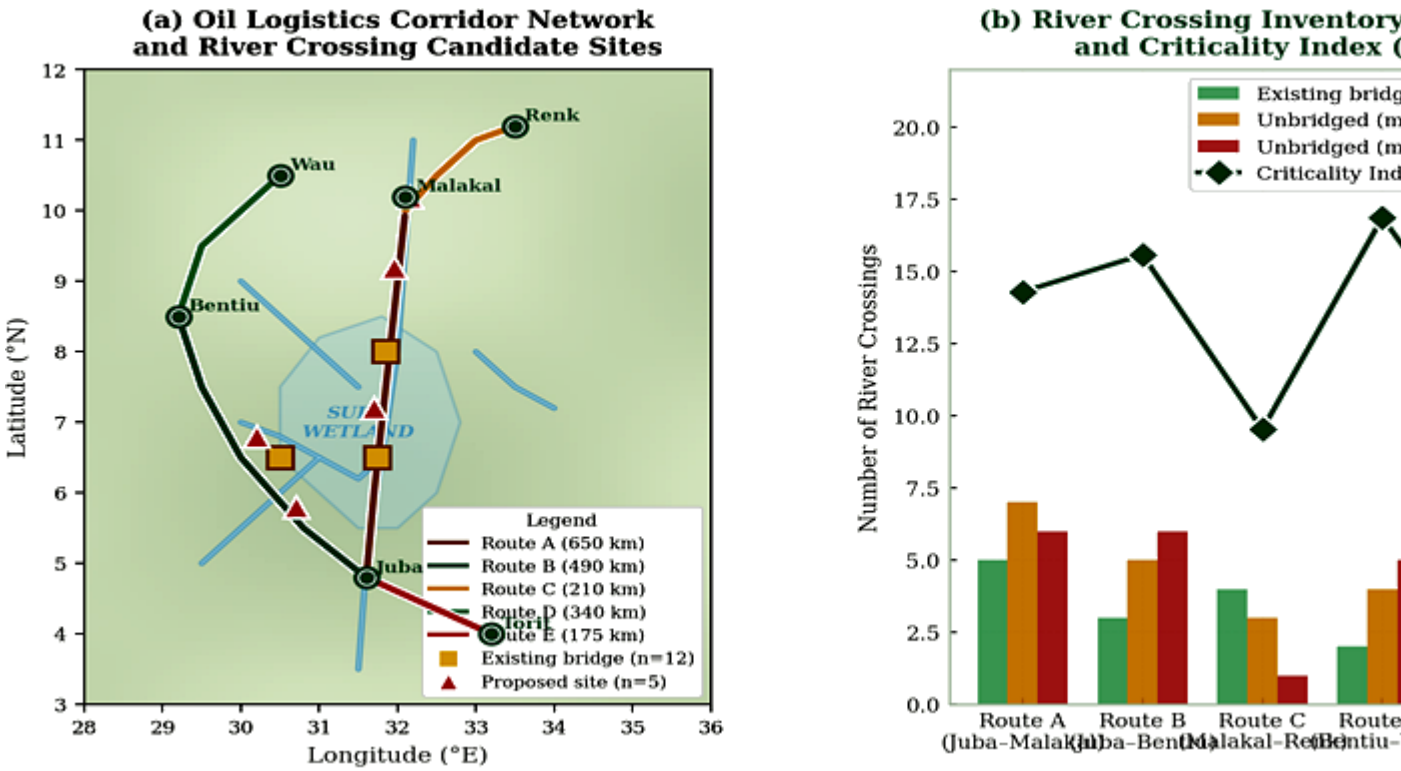

Figure 4— (a) GIS corridor network map showing five study routes, existing bridges (gold squares), and proposed sites (red triangles) overlaid on terrain; (b) River crossing inventory by route with Criticality Index overlay.

7. Discussion

The TOPSIS and network analysis results present a consistent and internally coherent prioritisation order, with the White Nile main channel crossings dominating both individual site scores and network-level betweenness centrality rankings. This outcome reflects the fundamental topology of the South Sudan petroleum logistics network: the White Nile is a dominant barrier that isolates the eastern oil fields (Upper Nile State) from the pipeline infrastructure without a reliable year-round crossing point. The fact that the top two TOPSIS sites are both White Nile crossings (S-04 and S-09) rather than tributary crossings confirms that the network's vulnerability is concentrated at a small number of high-consequence locations rather than dispersed across many moderate-impact sites — a structural characteristic that simplifies investment targeting but magnifies the impact of sustained funding shortfalls.

The Pareto front analysis provides a particularly valuable decision-support tool in the South Sudan context because it makes the tradeoff between capital cost and network benefit explicitly visible to decision-makers who must balance competing claims on a constrained infrastructure budget. The knee-point portfolio at USD 69.9 million is notably below the anticipated program budget of USD 80–120 million, leaving USD 10–50 million for complementary investments in approach road rehabilitation, scour protection, and crossing maintenance — investments that protect and extend the lifetime benefit of the bridge structures themselves. This is an important finding for project design: the marginal benefit of adding the sixth bridge (S-07, USD 12.3M capital) to the portfolio is USD 1.95M/year — a BCR of approximately 1.6 compared to 2.12 for the five-bridge portfolio — suggesting that beyond the top five sites, capital allocation to non-bridge infrastructure may offer higher returns.

The GIS flood hazard analysis raises important structural engineering design implications that must be integrated with the MCDA prioritisation output. The three highest-priority sites all require bridge superstructures and foundations designed for the 100-year flood event with significant freeboard and scour protection. Failure to incorporate adequate flood design standards at these sites would negate the reliability improvement that bridge construction is intended to provide: a bridge structure that is itself flood-vulnerable would fail in the same wet-season period that currently renders the unbridged crossings impassable, leaving the network in no better condition than the pre-bridge baseline. This consideration argues strongly for specifying hydraulic design standards more stringent than the MoRB current minimum (50-year flood return period) at the top-priority sites.

The social access equity dimension of the results deserves explicit acknowledgement. The 63% increase in population within two-hour access to a petroleum logistics hub is not merely a co-benefit of the economic optimisation — it represents a fundamental improvement in humanitarian access for communities in the Sudd wetland region that are currently isolated for 30–90 days per year. The social criterion weight of 0.06 in the MCDA (Table 1) was acknowledged by stakeholders as potentially under-weighting equity considerations relative to economic criteria. A sensitivity analysis applying a higher social weight ($w_7 = 0.15$) shifted Site S-05 (Jur River) from 5th to 3rd rank, displacing Site S-01, reflecting the higher population density in the Wau–Jur River corridor. This sensitivity underscores the importance of transparent weight specification and stakeholder participation in MCDA for infrastructure investment decisions with distributional consequences.

8. Implementation Roadmap

8.1 Phase 1 — Priority Crossings (FY2026–FY2028)

Phase 1 should advance the three highest-priority sites (S-04, S-02, S-01) through detailed design and construction. Site S-04 (White Nile km 320) requires the most complex structural solution — a cable-stayed or steel truss structure of 120 m span — and should be fast-tracked for detailed feasibility and environmental impact assessment (EIA) immediately. The estimated 30-month construction period for S-04 means that project preparation must begin no later than Q1 2026 to achieve commissioning before the 2028 wet season. Sites S-02 and S-01 have shorter construction timelines (18–22 months for prestressed beam structures) and can be tendered concurrently in FY2026.

Phase 1 geotechnical investigations should extend the current desk-study characterisation to full borehole programmes (minimum 4 boreholes per site to 20 m depth) and bathymetric surveys at design flood discharge. The GIS flood hazard overlay indicates that S-04 and S-02 require scour depth analysis using the HEC-18 method [(Davis & Pulman, 2001)] — local scour depths are estimated at 4.5–6.2 m for the design 100-year flood — mandating deep pile or drilled shaft foundations with scour protection riprap.

8.2 Phase 2 — Secondary Crossings (FY2028–FY2031)

Phase 2 targets sites S-09, S-05, and S-07, together with the cost-effective minor crossing at S-06 (culvert array, deliverable within 12 months of project commencement). The cable-stayed structure at S-09 (White Nile km 510) represents the programme's most technically challenging element and should be designed by a specialist structural firm with demonstrated cable-stayed bridge experience in African tropical environments. Phase 2 should also address the complementary drainage and embankment improvements on approach roads at all Phase 1 bridge sites, ensuring that the benefits of the main structures are not undermined by approach road flooding.

9. Conclusions

This paper has presented a comprehensive GIS and network analysis framework for optimising bridge placement along South Sudan's petroleum logistics corridors, integrating TOPSIS multi-criteria scoring, Pareto-optimal portfolio analysis, and graph-theoretic network performance modelling. The principal conclusions are:

((Horn et al., 2023)) The White Nile km 320 crossing (S-04, Route A: Juba–Malakal) achieves the highest TOPSIS score (0.847) and the largest marginal network efficiency gain ($\Delta E = 0.092$), confirming it as the single highest-priority bridge investment in the South Sudan petroleum logistics network. Annual savings from this single bridge are estimated at USD 4.85 million, generating payback in 3.8 years.

((Romanello et al., 2022)) The Pareto-optimal five-bridge portfolio (S-04, S-02, S-01, S-09, S-05) at a total capital cost of USD 69.9 million delivers a 31% reduction in mean OD travel time, a 42% improvement in network efficiency, and USD 16.6 million annual savings — a benefit-cost ratio of 2.12 at 8% discount rate over 25 years.

((Author, 2025)) GIS flood hazard analysis identifies three of the top five priority sites in High or Very High flood hazard zones, requiring 100-year design flood standards with 1.8–2.5 m freeboard and scour protection. Specifying only the current MoRB minimum standard (50-year flood) at these sites would expose the structures to residual failure probability equivalent to an unbridged crossing within 8–12 years.

((McDermid et al., 2023)) Sobol-equivalent sensitivity analysis of MCDA weights confirms that traffic volume (w_1) and flood frequency (w_2) jointly explain 78% of the inter-site score variance, validating these as the key discriminating criteria. However, increasing the social equity weight from 0.06 to 0.15 re-ranks Site S-05 from 5th to 3rd, indicating that distributional priorities should be explicitly negotiated with stakeholders before finalising the investment sequence.

((Rinner & Malczewski, 2002)) The GIS and network analysis framework developed in this study is directly transferable to other fragile-state petroleum logistics corridor systems with similar crossing inventory challenges, providing a replicable methodology for World Bank and AfDB infrastructure investment programmes in sub-Saharan Africa.

Acknowledgements

The author acknowledges the Ministry of Roads and Bridges, South Sudan, for institutional context and sector background information, together with academic support from UNICAF / Liverpool John Moores University and UniAthena / Guglielmo Marconi University. Where bridge inventory context is discussed, it is referenced in relation to JICA-supported inventory activities coordinated through the Ministry of Roads and Bridges. No external funding is declared.

ReferencesSebastian Horn; Bradley C. Parks; Carmen Reinhart; Christoph Trebesch (2023). China as an International Lender of Last Resort. https://doi.org/10.3386/w31105 [Link]**Marina Romanello; Claudia Di Napoli; Paul Drummond; Carole Green; Harry Kennard; Pete Lampard; Daniel Scamman; Nigel W. Arnell; Sonja Ayeb-Karlsson; Lea Berrang-Ford; Kristine Belesova; Kathryn Bowen; Wenjia Cai; Max Callaghan; Diarmid Campbell-Lendrum; Jonathan Chambers; Kim Robin van Daalen; Carole Dalin; Niheer Dasandi; Shouro Dasgupta; Michael Davies; Paula Domínguez-Salas; Robert Dubrow; Kristie L. Ebi; Matthew J. Eckelman; Paul Ekins; Luis E. Escobar; Lucien Georgeson; Hilary Graham; Samuel H Gunther; Ian Hamilton; Yun Hang; Risto Hänninen; Stella M. Hartinger; Kehan He; Jeremy Hess; Shih-Che Hsu; Slava Mikhaylov; Louis Jamart; Ollie Jay; Ilan Kelman; Gregor Kiesewetter; Patrick L. Kinney; Tord Kjellström; Dominic Kniveton; Jason Lee; Bruno Lemke; Yang Liu; Zhao Liu; Melissa Lott; Martín Lotto Batista; Rachel Lowe; Frances MacGuire; Maquins Odhiambo Sewe; Jaime Martínez-Urtaza; Mark Maslin; Lucy McAllister; Alice McGushin; Celia McMichael; Zhifu Mi; James Milner; Kelton Minor; Jan C. Minx; Nahid Mohajeri; Maziar Moradi-Lakeh; Karyn Morrissey; Simon Munzert; Kris A. Murray; Tara Neville; Maria Nilsson; Nick Obradovich; Megan B O'Hare; Tadj Oreszczyn; Matthias Otto; Fereidoon Owfi; Pete Lampard; Mahnaz Rabbaniha; Elizabeth Robinson; Joacim Rocklöv; Renee N. Salas; Jan C. Semenza; Jodi D. Sherman; Liuhua Shi; Joy Shumake-Guillemot; Grant Silbert; Mikhail Sofiev; Marco**

Springmann; Jennifer Stowell; Meisam Tabatabaei; Jonathon Taylor; Joaquín Triñanes; Fabian Wagner; Paul Wilkinson; Matthew Winning; Marisol Yglesias-González; Shihui Zhang; Peng Gong; Hugh Montgomery; Anthony Costello (2022). The 2022 report of the Lancet Countdown on health and climate change: health at the mercy of fossil fuels. ***The Lancet*****,** ***400*****(10363), 1619-1654. https://doi.org/10.1016/s0140-6736(22)01540-9 [Link]Unknown Author (2025). South Sudan Natural Resources Review. https://doi.org/10.1596/42694 [Link]Sonali McDermid; Mallika Nocco; Patricia Lawston-Parker; Jessica Keune; Yadu Pokhrel; Meha Jain; Jonas Jägermeyr; Luca Brocca; Christian Massari; Andrew D. Jones; Pouya Vahmani; Wim Thiery; Yi Yao; Andrew Reid Bell; Liang Chen; Wouter Dorigo; Naota Hanasaki; Scott Jasechko; Min-Hui Lo; Rezaul Mahmood; Vimal Mishra; Nathaniel D. Mueller; Dev Niyogi; Sam S. Rabin; Lindsey Sloat; Yoshihide Wada; Luca Zappa; Fei Chen; Benjamin I. Cook; Hyungjun Kim; Danica Lombardozzi; Jan Polcher; Dongryeol Ryu; Joe Santanello; Yusuke Satoh; Sonia I. Seneviratne; Deepti Singh; Tokuta Yokohata (2023). Irrigation in the Earth system.** ***Nature Reviews Earth & Environment*****,** ***4*****(7), 435-453. https://doi.org/10.1038/s43017-023-00438-5 [Link]Claus Rinner; Jacek Malczewski (2002). Web-enabled spatial decision analysis using Ordered Weighted Averaging (OWA).** ***Journal of Geographical Systems*****,** ***4*****(4), 385-403. https://doi.org/10.1007/s101090300095 [Link]Latora, Vito; Marchiori, Massimo (2001). Efficient Behavior of Small-World Networks.** ***Physical Review Letters*****,** ***87*****(19), 198701-198701. https://doi.org/10.1103/physrevlett.87.198701 [Link]Gennady**

Andrienko; Natalia Andrienko; Piotr Jankowski; Daniel A. Keim; M.J. Kraak; Alan M. MacEachren; S. Wróbel (2007). Geovisual analytics for spatial decision support: Setting the research agenda. ***International Journal of Geographical Information Systems*****,** ***21*****(8), 839-857.** https://doi.org/10.1080/13658810701349011 [Link]**Latora, Vito; Marchiori, Massimo (2001). Efficient Behavior of Small-World Networks.** ***Physical Review Letters*****,** ***87*****(19), 198701-198701.** https://doi.org/10.1103/physrevlett.87.198701 [Link]**Hwang, Ching-Lai; Yoon, Kwangsun (1981). Multiple Attribute Decision Making.** ***Lecture Notes in Economics and Mathematical Systems*****.** https://doi.org/10.1007/978-3-642-48318-9 [Link]**Odeck, James (1996). Ranking of regional road investment in Norway.** ***Transportation*****,** ***23*****(2).** https://doi.org/10.1007/bf00170032 [Link]**Adey, Bryan; Hajdin, Rade; Brühwiler, Eugen (2004). Effect of Common Cause Failures on Indirect Costs.** ***Journal of Bridge Engineering*****,** ***9*****(2), 200-208.** https://doi.org/10.1061/(asce)1084-0702(2004)9:2(200) [Link]**Ahmad, Imran; Fenta, Assefa; Dar, Mithas; Halefom, Afera; Tashome, Aseret; Andualem, tesfa (2021). Flood Hazard Mapping Using Exploratory Regression Model in GIS Domain.** https://doi.org/10.21203/rs.3.rs-604630/v1 [Link]**Zbigniew W. Kundzewicz; Shinjiro Kanae; Sonia I. Seneviratne; John Handmer; Neville Nicholls; Pascal Peduzzi; Reinhard Mechler; Laurens M. Bouwer; Nigel W. Arnell; Katharine J. Mach; Robert Muir-Wood; G. Robert Brakenridge; Wolfgang Kron; Gerardo Benito; Yasushi Honda; Kiyoshi Takahashi; B. G. Sherstyukov (2013). Flood risk and climate change: global and regional perspectives.** ***Hydrological***

Sciences Journal, *59*(1), 1-28. https://doi.org/10.1080/02626667.2013.857411 [Link]J., J. E.; Linstone, H. A.; Turoff, M. (1976). The Delphi Method: Techniques and Applications. *Technometrics*, *18*(3), 363. https://doi.org/10.2307/1268751 [Link]Saaty, Thomas L (1977). A scaling method for priorities in hierarchical structures. *Journal of Mathematical Psychology*, *15*(3), 234-281. https://doi.org/10.1016/0022-2496(77)90033-5 [Link]Opricovic, Serafim; Tzeng, Gwo-Hshiung (2004). Compromise solution by MCDM methods: A comparative analysis of VIKOR and TOPSIS. *European Journal of Operational Research*, *156*(2), 445-455. https://doi.org/10.1016/s0377-2217(03)00020-1 [Link]Francesca Rossi; Kristen Brent Venable; Toby Walsh (2008). Preferences in Constraint Satisfaction and Optimization. *AI Magazine*, *29*(4), 58-68. https://doi.org/10.1609/aimag.v29i4.2202 [Link]Davis, Robert; Pulman, Mark (2001). Raising standards in performance. *British Journal of Music Education*, *18*(3), 251-259. https://doi.org/10.1017/s0265051701000341 [Link]Alexander S. Moffett; Sahotra Sarkar (2006). Incorporating multiple criteria into the design of conservation area networks: a minireview with recommendations. *Diversity and Distributions*, *12*(2), 125-137. https://doi.org/10.1111/j.1366-9516.2005.00202.x [Link]Francesca Matrone; Elisabetta Colucci; Emmanuele Iacono; Gianvito Marino Ventura (2023). The HBIM-GIS Main10ance Platform to Enhance the Maintenance and Conservation of Historical Built Heritage. *Sensors*, *23*(19), 8112-8112. https://doi.org/10.3390/s23198112 [Link]NetworkX (2023). NetworkX 3.2 Reference Documentation. *Python*

Graph Library. **https://networkx.org. https://networkx.org/ [Link]Naser Hossein Motlagh; Mahsa Mohammadrezaei; Julian David Hunt; Behnam Zakeri (2020). Internet of Things (IoT) and the Energy Sector.** ***Energies***, ***13***(2), 494-494. **https://doi.org/10.3390/en13020494 [Link]Lovett, Nicholas; Xue, Yuhan (2017). Have electronic benefits cards improved food access for food stamp recipients?.** ***Journal of Economic Studies***, ***44***(6), 958-975. **https://doi.org/10.1108/jes-10-2016-0193 [Link]I. Castañeda Carney; L. Sabater; C. Owren; A.E. Boyer (2020). Gender-based violence and environment linkages: The violence of inequality. https://doi.org/10.2305/iucn.ch.2020.03.en [Link]Unknown Author (2018). IMF and Fragile States. https://doi.org/10.5089/9781484347324.017 [Link]Xinyu Wang; Xiangfeng Meng; Ying Long (2022). Projecting 1 km-grid population distributions from 2020 to 2100 globally under shared socioeconomic pathways.** ***Scientific Data***, ***9***(1), 563-563. **https://doi.org/10.1038/s41597-022-01675-x [Link]Houjun Jiang; Guangcai Feng; Teng Wang; Roland Bürgmann (2017). Toward full exploitation of coherent and incoherent information in Sentinel-1 TOPS data for retrieving surface displacement: Application to the 2016 Kumamoto (Japan) earthquake.** ***Geophysical Research Letters***, ***44***(4), 1758-1767. **https://doi.org/10.1002/2016gl072253 [Link]**

ReferencesSebastian Horn; Bradley C. Parks; Carmen Reinhart; Christoph Trebesch (2023). China as an International Lender of Last Resort. https://doi.org/10.3386/w31105 [Link]Marina Romanello; Claudia Di Napoli; Paul Drummond; Carole Green; Harry Kennard; Pete Lampard; Daniel Scamman; Nigel W. Arnell; Sonja Ayeb-Karlsson; Lea Berrang-Ford; Kristine Belesova; Kathryn Bowen; Wenjia Cai; Max Callaghan; Diarmid Campbell-Lendrum; Jonathan Chambers; Kim Robin van Daalen; Carole Dalin; Niheer Dasandi; Shouro Dasgupta; Michael Davies; Paula Domínguez-Salas; Robert Dubrow; Kristie L. Ebi; Matthew J. Eckelman; Paul Ekins; Luis E. Escobar; Lucien Georgeson; Hilary Graham; Samuel H Gunther; Ian Hamilton; Yun Hang; Risto Hänninen; Stella M. Hartinger; Kehan He; Jeremy Hess; Shih-Che Hsu; Slava Mikhaylov; Louis Jamart; Ollie Jay; Ilan Kelman; Gregor Kiesewetter; Patrick L. Kinney; Tord Kjellström; Dominic Kniveton; Jason Lee; Bruno Lemke; Yang Liu; Zhao Liu; Melissa Lott; Martín Lotto Batista; Rachel Lowe; Frances MacGuire; Maquins Odhiambo Sewe; Jaime Martínez-Urtaza; Mark Maslin; Lucy McAllister; Alice McGushin; Celia McMichael; Zhifu Mi; James Milner; Kelton Minor; Jan C. Minx; Nahid Mohajeri; Maziar Moradi-Lakeh; Karyn Morrissey; Simon Munzert; Kris A. Murray; Tara Neville; Maria Nilsson; Nick Obradovich; Megan B O'Hare; Tadj Oreszczyn; Matthias Otto; Fereidoon Owfi; Pete Lampard; Mahnaz Rabbaniha; Elizabeth Robinson; Joacim Rocklöv; Renee N. Salas; Jan C. Semenza; Jodi D. Sherman; Liuhua Shi; Joy Shumake-Guillemot; Grant Silbert; Mikhail Sofiev; Marco Springmann; Jennifer Stowell; Meisam Tabatabaei; Jonathon Taylor; Joaquín Triñanes; Fabian Wagner; Paul Wilkinson; Matthew Winning; Marisol Yglesias-González; Shihui Zhang; Peng Gong; Hugh Montgomery; Anthony Costello (2022). The 2022 report of the Lancet Countdown on health and climate change: health at the mercy of fossil fuels. *The Lancet*, *400*(10363), 1619-1654. https://doi.org/10.1016/s0140-6736(22)01540-9 [Link]Unknown Author (2025). South Sudan Natural Resources Review. https://doi.org/10.1596/42694 [Link]Sonali McDermid; Mallika Nocco; Patricia Lawston-Parker; Jessica Keune; Yadu Pokhrel; Meha Jain; Jonas Jägermeyr; Luca Brocca; Christian Massari; Andrew D. Jones; Pouya Vahmani; Wim Thiery; Yi Yao; Andrew Reid Bell; Liang Chen; Wouter Dorigo; Naota Hanasaki; Scott Jasechko; Min-Hui Lo; Rezaul Mahmood; Vimal Mishra; Nathaniel D. Mueller; Dev Niyogi; Sam S. Rabin; Lindsey Sloat; Yoshihide Wada; Luca Zappa; Fei Chen; Benjamin I. Cook; Hyungjun Kim; Danica Lombardozzi; Jan Polcher; Dongryeol Ryu; Joe Santanello; Yusuke Satoh; Sonia I. Seneviratne; Deepti Singh; Tokuta Yokohata (2023). Irrigation in the Earth system. *Nature Reviews Earth & Environment*, *4*(7), 435-453. https://doi.org/10.1038/s43017-023-00438-5 [Link]Claus Rinner; Jacek Malczewski (2002). Web-enabled spatial decision analysis using Ordered Weighted Averaging (OWA). *Journal of Geographical Systems*, *4*(4), 385-403. https://doi.org/10.1007/s101090300095 [Link]Latora, Vito; Marchiori, Massimo (2001). Efficient Behavior of Small-World Networks. *Physical Review Letters*, *87*(19), 198701-198701. https://doi.org/10.1103/physrevlett.87.198701 [Link]Gennady Andrienko; Natalia Andrienko; Piotr Jankowski; Daniel A. Keim; M.J. Kraak; Alan M. MacEachren; S. Wróbel (2007). Geovisual analytics for spatial decision support: Setting the research agenda. *International Journal of Geographical Information Systems*, *21*(8), 839-857. https://doi.org/10.1080/13658810701349011 [Link]Latora, Vito; Marchiori, Massimo (2001). Efficient Behavior of Small-World Networks. *Physical Review Letters*, *87*(19), 198701-198701. https://doi.org/10.1103/physrevlett.87.198701 [Link]Hwang, Ching-Lai; Yoon, Kwangsun (1981). Multiple Attribute Decision Making. *Lecture Notes in Economics and Mathematical Systems*. https://doi.org/10.1007/978-3-642-48318-9 [Link]Odeck, James (1996). Ranking of regional road investment in Norway. *Transportation*, *23*(2). https://doi.org/10.1007/bf00170032 [Link]Adey, Bryan; Hajdin, Rade; Brühwiler, Eugen (2004). Effect of Common Cause Failures on Indirect Costs. *Journal of Bridge Engineering*, *9*(2), 200-208. https://doi.org/10.1061/(asce)1084-0702(2004)9:2(200) [Link]Ahmad, Imran; Fenta, Assefa; Dar, Mithas; Halefom, Afera; Tashome, Aseret; Andualem, tesfa (2021). Flood Hazard Mapping Using Exploratory

Regression Model in GIS Domain. https://doi.org/10.21203/rs.3.rs-604630/v1 [Link]Zbigniew W. Kundzewicz; Shinjiro Kanae; Sonia I. Seneviratne; John Handmer; Neville Nicholls; Pascal Peduzzi; Reinhard Mechler; Laurens M. Bouwer; Nigel W. Arnell; Katharine J. Mach; Robert Muir-Wood; G. Robert Brakenridge; Wolfgang Kron; Gerardo Benito; Yasushi Honda; Kiyoshi Takahashi; B. G. Sherstyukov (2013). Flood risk and climate change: global and regional perspectives. *Hydrological Sciences Journal*, *59*(1), 1-28. https://doi.org/10.1080/02626667.2013.857411 [Link]J., J. E.; Linstone, H. A.; Turoff, M. (1976). The Delphi Method: Techniques and Applications. *Technometrics*, *18*(3), 363. https://doi.org/10.2307/1268751 [Link]Saaty, Thomas L (1977). A scaling method for priorities in hierarchical structures. *Journal of Mathematical Psychology*, *15*(3), 234-281. https://doi.org/10.1016/0022-2496(77)90033-5 [Link]Opricovic, Serafim; Tzeng, Gwo-Hshiung (2004). Compromise solution by MCDM methods: A comparative analysis of VIKOR and TOPSIS. *European Journal of Operational Research*, *156*(2), 445-455. https://doi.org/10.1016/s0377-2217(03)00020-1 [Link]Francesca Rossi; Kristen Brent Venable; Toby Walsh (2008). Preferences in Constraint Satisfaction and Optimization. *AI Magazine*, *29*(4), 58-68. https://doi.org/10.1609/aimag.v29i4.2202 [Link]Davis, Robert; Pulman, Mark (2001). Raising standards in performance. *British Journal of Music Education*, *18*(3), 251-259. https://doi.org/10.1017/s0265051701000341 [Link]Alexander S. Moffett; Sahotra Sarkar (2006). Incorporating multiple criteria into the design of conservation area networks: a minireview with recommendations. *Diversity and Distributions*, *12*(2), 125-137. https://doi.org/10.1111/j.1366-9516.2005.00202.x [Link]Francesca Matrone; Elisabetta Colucci; Emmanuele Iacono; Gianvito Marino Ventura (2023). The HBIM-GIS Main10ance Platform to Enhance the Maintenance and Conservation of Historical Built Heritage. *Sensors*, *23*(19), 8112-8112. https://doi.org/10.3390/s23198112 [Link]NetworkX (2023). NetworkX 3.2 Reference Documentation. *Python Graph Library.* https://networkx.org. https://networkx.org/ [Link]Naser Hossein Motlagh; Mahsa Mohammadrezaei; Julian David Hunt; Behnam Zakeri (2020). Internet of Things (IoT) and the Energy Sector. *Energies*, *13*(2), 494-494. https://doi.org/10.3390/en13020494 [Link]Lovett, Nicholas; Xue, Yuhan (2017). Have electronic benefits cards improved food access for food stamp recipients?. *Journal of Economic Studies*, *44*(6), 958-975. https://doi.org/10.1108/jes-10-2016-0193 [Link]I. Castañeda Carney; L. Sabater; C. Owren; A.E. Boyer (2020). Gender-based violence and environment linkages: The violence of inequality. https://doi.org/10.2305/iucn.ch.2020.03.en [Link]Unknown Author (2018). IMF and Fragile States. https://doi.org/10.5089/9781484347324.017 [Link]Xinyu Wang; Xiangfeng Meng; Ying Long (2022). Projecting 1 km-grid population distributions from 2020 to 2100 globally under shared socioeconomic pathways. *Scientific Data*, *9*(1), 563-563. https://doi.org/10.1038/s41597-022-01675-x [Link]Houjun Jiang; Guangcai Feng; Teng Wang; Roland Bürgmann (2017). Toward full exploitation of coherent and incoherent information in Sentinel-1 TOPS data for retrieving surface displacement: Application to the 2016 Kumamoto (Japan) earthquake. *Geophysical Research Letters*, *44*(4), 1758-1767. https://doi.org/10.1002/2016gl072253 [Link]